Polarization effects in pion electroproduction from ³He

R.-W. Schulze* and P. U. Sauer

Institute for Theoretical Physics, University of Hannover, D-30167 Hannover, Germany

(Received 15 August 1996)

Inelastic electron scattering from ³He is studied in the kinematic region of pion production. Inclusive processes with polarization of the electron probe and of the ³He target are described in the plane wave impulse approximation. The question to what extent polarized ³He can serve in this kinematic regime as a substitute for unavailable neutron spin targets is discussed. [S0556-2813(97)02103-1]

I. INTRODUCTION

Pion production off nuclei will experimentally be studied at the continuous beam electron accelerators [1] with particular emphasis. This paper describes inclusive inelastic electron scattering from ³He in the region of pion production. Theoretical predictions for spin-averaged and spin-dependent structure functions are made. In particular, the question is discussed if polarized ³He can reliably serve as a substitute for otherwise unavailable neutron spin targets [2]. This question got a rather pessimistic answer in Ref. [3] for neutron charge properties at small momentum transfers to be seen in quasielastic scattering; it will get a positive answer for pion production. The paper assumes the nucleus to consist of nucleons only. Thus, it entirely misses the discussion [4] to what extent pion production in electromagnetic (e.m.) processes could determine a possible Δ-isobar content of the trinucleon bound states.

The paper employs the plane-wave impulse approximation (PWIA) for the description of inelastic electron scattering [3,5–7]. PWIA relates the nuclear structure functions to the nucleonic ones. The inclusive cross section is given in terms of the nuclear structure functions. The theoretical apparatus is taken over from Refs. [3] and [6]; Ref. [8] contains the preliminary results presented in this paper. Section II recalls the essential elements of PWIA. Section III presents a crude field-theoretic model for pion production from the single nucleon; it yields the parametrization of the nucleonic structure functions required for the present calculation. Section IV shows results for the ³He structure functions; it investigates to what extent neutron structure functions can be extracted from measured ³He structure functions.

II. PWIA FOR PION PRODUCTION FROM ³HE

The inclusive cross section of inelastic electron scattering from a target A with mass m_A, four-momentum P_A, and polarization n_A is determined by the nuclear current tensor $W_A^{\mu\nu}(Q,P_A)$. The four-vectors P_A and n_A satisfy the constraints $P_A^2 = m_A^2$, $n_A^2 = -1$, and $P_A \cdot n_A = 0$. For a spin-$\frac{1}{2}$ target the current tensor has the general form

___

*Present address: Scandpower GmbH, Flotowstraβe 41-43, D-22083 Hamburg, Germany.

$$\langle n_A | W_A^{\mu\nu}(Q,P_A) | n_A \rangle$$

$$= \left[\frac{Q^\mu Q^\nu}{Q^2} - g^{\mu\nu} \right] W_1^A(Q^2, Q \cdot P_A / m_A)$$

$$+ \widetilde{P}_A^\mu \widetilde{P}_A^\nu \frac{W_2^A(Q^2, Q \cdot P_A / m_A)}{m_A^2}$$

$$+ i \epsilon^{\mu\nu\alpha\beta} Q_\alpha \left[n_{A\beta} \frac{G_1^A(Q^2, Q \cdot P_A / m_A)}{m_A} \right.$$

$$+ [(Q \cdot P_A) n_{A\beta} - (Q \cdot n_A) P_{A\beta}]$$

$$\left. \times \frac{G_2^A(Q^2, Q \cdot P_A / m_A)}{m_A^3} \right]; \tag{2.1}$$

Q is the momentum transfer to the nucleus, $\widetilde{P}_A$, i.e.,

$$\widetilde{P}_A := P_A - \frac{Q \cdot P_A}{Q^2} Q, \tag{2.2}$$

the target momentum orthogonalized to Q. In Eq. (2.1) $g^{\mu\nu}$ is the ordinary metric tensor with $g^{00} = -g^{11} = -g^{22} = -g^{33} = 1$ and $\epsilon^{\mu\nu\alpha\beta}$ the totally antisymmetric tensor of dimension four with $\epsilon_{0123} = -\epsilon^{0123} = 1$. The notation $\langle n_A | W_A^{\mu\nu}(Q,P_A) | n_A \rangle$ indicates that the current tensor $W_A^{\mu\nu}(Q,P_A)$ is an operator in the nuclear spin space.

The spin-averaged structure functions W_i^A and the spin-dependent structure functions G_i^A determine the nuclear current tensor and therefore the inclusive cross section. They are real Lorentz scalars depending on the scalars Q^2 and $Q \cdot P_A$. The dependence of the current tensor on the polarization vector n_A is at most linear for a spin-$\frac{1}{2}$ nucleus. In the parametrization of the current tensor (2.1) the dependence on the pseudoscalar $Q \cdot n_A$ is explicitly split off from the structure functions.

The structure functions are obtained from a given current tensor by contractions with kinematic tensors. The relations are given explicitly in Ref. [3]. Without lack of generality, we carry out the calculation for a target at rest. The three four-vectors which determine the Lorentz structure of the current tensor are chosen as

$$P_A = (m_A, \mathbf{0}), \tag{2.3a}$$

$$n_A = (0, n_A^1, 0, n_A^3), \tag{2.3b}$$

$$Q = (Q^0, 0, 0, |\mathbf{Q}|). \tag{2.3c}$$

The polarization vector n_A is spacelike and therefore does not carry any time component, since $P_A \cdot n_A = 0$. The unit vectors $\hat{\mathbf{e}}_i$ of the nuclear c.m. system are defined by

$$\hat{\mathbf{e}}_3 = \hat{\mathbf{Q}}, \tag{2.4a}$$

$$\hat{\mathbf{e}}_2 = \frac{(\hat{\mathbf{e}}_3 \times \hat{\mathbf{n}}_A)}{|\hat{\mathbf{e}}_3 \times \hat{\mathbf{n}}_A|}, \tag{2.4b}$$

$$\hat{\mathbf{e}}_1 = \hat{\mathbf{e}}_2 \times \hat{\mathbf{e}}_3. \tag{2.4c}$$

In this c.m. system the scalar relations for the structure functions resulting from contractions of the current tensor with kinematic tensors take the particular forms

$$W_1^A(Q^2, Q \cdot P_A / m_A) = \frac{1}{2} \langle n_A | W_A^{11}(Q, P_A) + W_A^{22}(Q, P_A) | n_A \rangle, \tag{2.5a}$$

$$W_2^A(Q^2, Q \cdot P_A / m_A) = \frac{Q^4}{\mathbf{Q}^4} \langle n_A | W_A^{00}(Q, P_A) | n_A \rangle$$
$$- \frac{1}{2} \frac{Q^2}{\mathbf{Q}^2} \langle n_A | W_A^{11}(Q, P_A)$$
$$+ W_A^{22}(Q, P_A) | n_A \rangle, \tag{2.5b}$$

$$G_1^A(Q^2, Q \cdot P_A / m_A) = -\frac{i}{2} \frac{m_A^2}{\mathbf{Q}^2} \left[\frac{1}{n_A^1} \frac{Q^2}{m_A |\mathbf{Q}|} \langle n_A | W_A^{02}(Q, P_A) \right.$$
$$- W_A^{20}(Q, P_A) | n_A \rangle$$
$$+ \frac{1}{n_A^3} \frac{Q^0}{m_A} \langle n_A | W_A^{12}(Q, P_A)$$
$$\left. - W_A^{21}(Q, P_A) | n_A \rangle \right], \tag{2.5c}$$

$$G_2^A(Q^2, Q \cdot P_A / m_A) = \frac{i}{2} \frac{m_A^2}{\mathbf{Q}^2} \left[\frac{1}{n_A^1} \frac{Q^0}{|\mathbf{Q}|} \langle n_A | W_A^{02}(Q, P_A) \right.$$
$$- W_A^{20}(Q, P_A) | n_A \rangle$$
$$\left. + \frac{1}{n_A^3} \langle n_A | W_A^{12}(Q, P_A) - W_A^{21}(Q, P_A) | n_A \rangle \right]. \tag{2.5d}$$

For the results (2.5) current conservation is employed in order to eliminate the third components of the current tensor by the zero components, i.e.,

$$W_A^{3\nu}(Q, P_A) = \frac{Q^0}{|\mathbf{Q}|} W_A^{0\nu}(Q, P_A), \tag{2.6a}$$

$$W_A^{\mu 3}(Q, P_A) = \frac{Q^0}{|\mathbf{Q}|} W_A^{\nu 0}(Q, P_A). \tag{2.6b}$$

The results (2.5) are unique as long as the current tensor is covariant and respects current conservation. In contrast, the current tensor to be calculated in this paper by PWIA is only approximate. Reference [3] discusses the ensuing theoretical problems; it calls the results (2.5) the extraction scheme (A) which Refs. [3] and [6] have reasons to favor and which will be used exclusively in this paper.

In the nuclear c.m. system the structure functions are related to the nuclear response functions by

$$W_1^A(Q^2, Q \cdot P_A / m_A) = \frac{1}{2} R_T^A(Q^2, Q^0), \tag{2.7a}$$

$$W_2^A(Q^2, Q \cdot P_A / m_A) = \frac{Q^4}{\mathbf{Q}^4} R_L^A(Q^2, Q^0) - \frac{1}{2} \frac{Q^2}{\mathbf{Q}^2} R_T^A(Q^2, Q^0), \tag{2.7b}$$

$$G_1^A(Q^2, Q \cdot P_A / m_A) = \frac{1}{2} \frac{m_A^2}{\mathbf{Q}^2} \left[\frac{Q^2}{m_A |\mathbf{Q}|} \sqrt{\frac{1}{2}} R_{TL'}^A(Q^2, Q^0) \right.$$
$$\left. + \frac{Q^0}{m_A} R_{T'}^A(Q^2, Q^0) \right], \tag{2.7c}$$

$$G_2^A(Q^2, Q \cdot P_A / m_A) = -\frac{1}{2} \frac{m_A^2}{\mathbf{Q}^2} \left[\frac{Q^0}{|\mathbf{Q}|} \sqrt{\frac{1}{2}} R_{TL'}^A(Q^2, Q^0) \right.$$
$$\left. + R_{T'}^A(Q^2, Q^0) \right]. \tag{2.7d}$$

We carry out the calculation for structure functions. However, in the context of physics discussions we shall use structure functions and response functions interchangeably: The response functions, i.e., the spin-averaged longitudinal and transverse responses R_L^A and R_T^A and the spin-dependent transverse and transverse-longitudinal responses $R_{T'}^A$ and $R_{TL'}^A$ are directly related to the longitudinal and transverse components of the nuclear current four-vectors.

The nuclear responses determine the spin-dependent cross sections, i.e.,

$$\frac{d^2\sigma}{dk_e'^0 d\Omega_e'}(h_e, \hat{\mathbf{n}}_A) = \sigma_{\text{Mott}} \left(\frac{Q^4}{\mathbf{Q}^4} R_L^A(Q^2, \Omega) \right.$$
$$+ \left[-\frac{1}{2} \frac{Q^2}{\mathbf{Q}^2} + \tan^2 \frac{\Theta_e}{2} \right] R_T^A(Q^2, \Omega)$$
$$+ h_e \tan \frac{\Theta_e}{2} \left[\sqrt{-\frac{Q^2}{\mathbf{Q}^2} + \tan^2 \frac{\Theta_e}{2}} \right.$$
$$\times R_{T'}^A(Q^2, \Omega) \cos\theta^*$$
$$\left. \left. + \sqrt{\frac{1}{2} \frac{Q^2}{\mathbf{Q}^2}} R_{TL'}^A(Q^2, \Omega) \sin\theta^* \cos\phi^* \right] \right). \tag{2.8a}$$
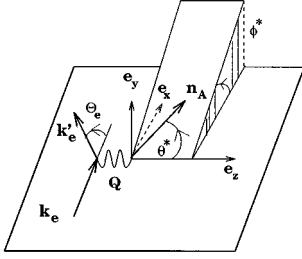
FIG. 1. Parametrization of the target polarization in terms of the angles (θ^*, ϕ^*). The electron carries the momentum k_e and k'_e before and after the collision. The shaded area lies in the x-y plane; the projection of $\mathbf{n}_A$ onto that plane forms the angle ϕ^* with the x direction. The spatial momentum transfer defines the z direction. The coordinate system $(\hat{\mathbf{e}}_x, \hat{\mathbf{e}}_y, \hat{\mathbf{e}}_z)$ is different from the system of Eq. (2.4) on which the calculation (2.5) is based; in the system (2.4) the polarization vector has the form $\hat{\mathbf{n}}_A = (\cos\theta^*, 0, \sin\theta^*)$.

The four-momentum of the electron in the final state is denoted by $k'_e = (|\mathbf{k}'_e|, |\mathbf{k}'_e| \Omega'_e)$ with Θ_e being the scattering angle; the energy loss of the electron is $\Omega = Q^0$, its helicity h_e. The Mott cross section

$$\sigma_{\text{Mott}} = \left(\frac{e_p^2}{8\pi k_e^0} \right)^2 \frac{\cos^2\Theta_e/2}{\sin^4\Theta_e/2} \qquad (2.8b)$$

is used, k_e^0 being the electron beam energy and e_p the proton charge. The polarization of the target is parametrized by the angles (θ^*, ϕ^*) as indicated in Fig. 1. In the particular coordinate system (2.4) on which the relations (2.5) for the structure functions are based the polarization vector n_A has the components $(0, \cos\theta^*, 0, \sin\theta^*)$.

We calculate the nuclear current tensor in PWIA, i.e.,

$$\langle n_A | W_A^{\mu\nu}(Q, P_A) | n_A \rangle$$

$$= \sum_{t_N} \int dE \int d^3 p_N \frac{m_N}{p_N^0}$$

$$\times \text{Tr}\left[W_{N(t_N)}^{\mu\nu}(Q_N, p_N) S(E\mathbf{p}_N t_N) \frac{1}{2}(1 + \hat{\mathbf{n}}_A \boldsymbol{\sigma}_A) \right]. \qquad (2.9)$$

PWIA is diagrammatically defined in Fig. 2. PWIA takes only the single-nucleon part of the nuclear current into account. Furthermore, it splits the hadronic final state up into a tensor product consisting of fully correlated states with $(A-1)$ nucleons and of the states with baryon number one, reached by the single-nucleon current, but possibly containing many particles due to inelastic excitation. The final-state interactions between the particles of the one-baryon state and the $(A-1)$-spectator system are neglected; for example, in pion production the produced pion does not undergo distortion by the nucleus. The assumptions of PWIA yield for the nuclear current tensor the convolution of the nucleonic current tensor $W_{N(t_N)}^{\mu\nu}(Q_N, p_N)$ with the spectral function $S(E\mathbf{p}_N t_N)$; the proton and neutron contributions add up incoherently. The isospin label t_N distinguishes between proton and neutron. The convolution formula (2.9) is derived in Ref.
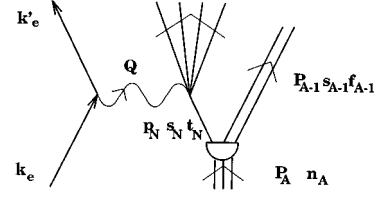

FIG. 2. Kinematics of inelastic electron scattering from a nucleus in PWIA. The electron carries the momentum k_e and k'_e before and after the collision. The target has the momentum P_A and the polarization n_A, the struck nucleon the momentum p_N, spin projection s_N, and isospin label t_N, and the $(A-1)$-spectator system the total momentum P_{A-1}, the quantum numbers of internal motion f_{A-1}. The momentum transfer to the nucleus by the electron is Q. In case of trinucleon targets the $(A-1)$-spectator systems are the deuteron and the two-nucleon scattering states.

[3]. It makes a distinction between the momentum transfers Q to the nucleus and Q_N to the nucleon. The struck nucleon is bound, carries three-momentum $\mathbf{p}_N$ and is assumed to be on its mass shell, i.e., $p_N^0 = \sqrt{m_N^2 + \mathbf{p}_N^2}$. The energy E is required to remove the nucleon from the nucleus with definite excitation of the $(A-1)$-spectator system. Thus, $Q_N = (Q^0 + Am_N - E - \sqrt{(A-1)^2 m_N^2 + \mathbf{p}_N^2} - p_N^0, \mathbf{Q})$. Denoting the nuclear spin operator with $\boldsymbol{\sigma}_A$, $(1 + \hat{\mathbf{n}}_A \cdot \boldsymbol{\sigma}_A)/2$ is the density operator; $\hat{\mathbf{n}}_A^2 = 1$ signals a pure target state what we assume. The nucleonic current tensor $W_{N(t_N)}^{\mu\nu}(Q_N, p_N)$ is an operator in nucleonic spin space with a spin structure corresponding to Eq. (2.1). The spectral function $S(E\mathbf{p}_N t_N)$ is an operator in nucleonic and nuclear spin space. The trace operation of Eq. (2.9) refers to nucleonic and nuclear spin. The spectral function $S(E\mathbf{p}_N t_N)$ contains all information on the target required for PWIA. Its particular form for the trinucleon bound state is discussed extensively in Ref. [3]; that discussion is not repeated here.

III. PARAMETRIZATION OF THE NUCLEONIC CURRENT TENSOR

The description of electropion production from ^{3}He in terms of the convolution relation (2.9) requires knowledge of the nucleonic current tensor $W_{N(t_N)}^{\mu\nu}(Q_N, p_N)$ in this kinematic regime. We use the crude field theoretic model of Ref. [6] for the current, but extend it to include polarization. The current model is diagrammatically defined in Fig. 3. It is based on the e.m. excitation of the nucleon to the Δ resonance, decaying into pion-nucleon states, and on nonresonant background processes, derived from pion-nucleon dynamics in pseudovector coupling. The nucleonic current tensor is obtained by calculating the four Lorentz-invariant nucleonic structure functions or, equivalently, the four nucleonic responses in the nucleonic c.m. system. The calculational procedure of the spin-averaged structure functions is described in Appendix C of Ref. [6]; its extension to the spin-dependent structure functions is straightforward.

The current model is tuned to account for the inclusive nucleon cross section for which data are only scarcely known. The cross section has the general form of Eq. (2.8a)
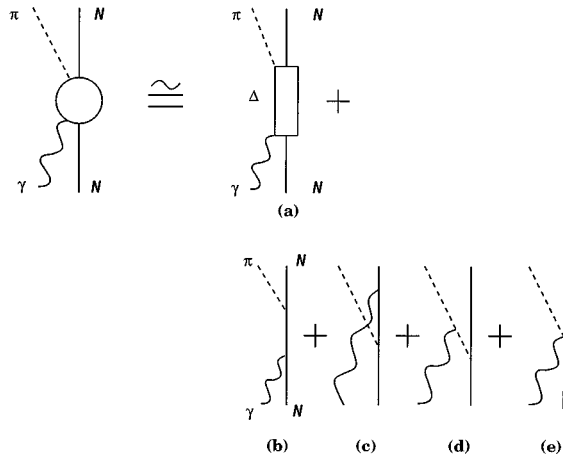
FIG. 3. Processes considered in the calculation of the electro-pion production amplitude. The full line denotes nucleons, the open rectangle the Δ isobar, the wavy line the e.m. current, and the dashed line the pion. In the process (a) pion production proceeds through the e.m. excitation of the Δ resonance in pion-nucleon scattering. Processes (b) to (e) are background processes for which Born approximation is used; they are based on pseudovector pion-nucleon coupling.

in the nucleonic rest frame which is traditionally rewritten as

$$\frac{d^2\sigma}{dk_e'^0 d\Omega_e'}(h_e,\hat{\mathbf{n}}_N) = \Gamma_e(\sigma_{\mathrm{T}}^{N(t_N)}(Q_N^2,\Omega_N) + \epsilon\sigma_{\mathrm{L}}^{N(t_N)}(Q_N^2,\Omega_N)$$
$$+ h_e(\sqrt{1-\epsilon^2}\sigma_{\mathrm{T}'}^{N(t_N)}(Q_N^2,\Omega_N)\cos\theta_N^*$$
$$+ \sqrt{2\epsilon(1-\epsilon^2)}\sigma_{\mathrm{TL}'}^{N(t_N)}$$
$$\times (Q_N^2,\Omega_N)\sin\theta_N^*\cos\phi_N^*)), \tag{3.1}$$

with

$$\Gamma_e := \sigma_{\mathrm{Mott}}\left[-\frac{Q_N^2}{2\mathbf{Q}_N^2} + \tan^2\frac{\Theta_e}{2}\right]\left[\frac{\Omega_N + Q_N^2/2m_N}{e_p^2\pi/2}\right], \tag{3.2a}$$

$$\epsilon := \left(1 - \frac{2\mathbf{Q}_N^2}{Q_N^2}\tan^2\frac{\Theta_e}{2}\right)^{-1}, \tag{3.2b}$$

and Ω_N being the energy loss $Q_N \cdot p_N/m_N = Q_N^0$ in the nucleonic rest frame, n_N describing the nucleonic polarization and having the components $(0,\cos\theta_N^*,0,\sin\theta_N^*)$. The unpolarized $(\sigma_{\mathrm{L}}^{N(t_N)},\sigma_{\mathrm{T}}^{N(t_N)})$ and the polarized partial cross sections $(\sigma_{\mathrm{T}'}^{N(t_N)},\sigma_{\mathrm{TL}'}^{N(t_N)})$ are directly related to the nucleonic response functions $R_i^{N(t_N)}, i=\mathrm{L,T,T',TL'}$, defined in correspondence to Eq. (2.7), by

$$\sigma_{\mathrm{T}}^{N(t_N)}(Q_N^2,\Omega_N) := \frac{e_p^2\pi/2}{\Omega_N + Q_N^2/2m_N}R_{\mathrm{T}}^{N(t_N)}(Q_N^2,\Omega_N), \tag{3.3a}$$
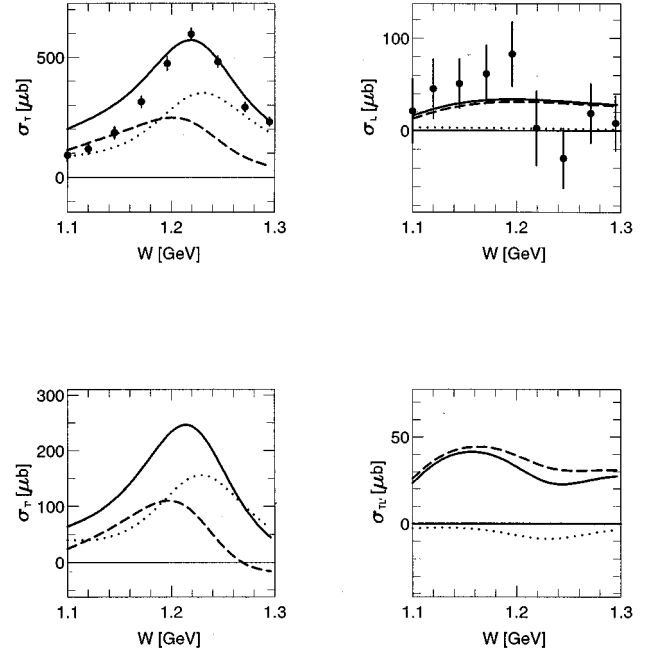

FIG. 4. Partial cross sections $\sigma_{\mathrm{T}}^p, \sigma_{\mathrm{L}}^p, \sigma_{\mathrm{T}'}^p$, and $\sigma_{\mathrm{TL}'}^p$ of inclusive scattering for pion production from the proton as function of the total pion-nucleon mass W, i.e., $W^2=(Q_N+p_N)^2$. The partial cross sections in the proton c.m. system refer to the four-momentum transfer $Q_N^2 = -0.20$ GeV^2; they are shown as solid curves. π^+ and π^0 production are indicated as dashed and dotted lines, respectively. The experimental data are taken from Ref. [9].

$$\sigma_{\mathrm{L}}^{N(t_N)}(Q_N^2,\Omega_N) := \frac{e_p^2\pi/2}{\Omega_N + Q_N^2/2m_N}R_{\mathrm{L}}^{N(t_N)}(Q_N^2,\Omega_N)\frac{-2Q_N^2}{\mathbf{Q}_N^2}, \tag{3.3b}$$

$$\sigma_{\mathrm{T}'}^{N(t_N)}(Q_N^2,\Omega_N) := \frac{e_p^2\pi/2}{\Omega_N + Q_N^2/2m_N}R_{\mathrm{T}'}^{N(t_N)}(Q_N^2,\Omega_N), \tag{3.3c}$$

$$\sigma_{\mathrm{TL}'}^{N(t_N)}(Q_N^2,\Omega_N) := \frac{e_p^2\pi/2}{\Omega_N + Q_N^2/2m_N}R_{\mathrm{TL}'}^{N(t_N)}(Q_N^2,\Omega_N)$$
$$\times (-)\sqrt{\frac{-Q_N^2}{2\mathbf{Q}_N^2}}. \tag{3.3d}$$

The response functions and the partial cross sections are frame dependent and no Lorentz scalars. In Fig. 4 predictions for the four partial cross sections $\sigma_{\mathrm{L}}^p, \sigma_{\mathrm{T}}^p, \sigma_{\mathrm{T}'}^p$, and $\sigma_{\mathrm{TL}'}^p$ of inclusive scattering from the proton are shown, with p standing for the label $N(1/2)$; the contributions arising from π^+ and π^0 production are separately given. When possible, the predictions are compared with experimental data [9]. A corresponding calculation of electropion production on the single nucleon has been presented in Ref. [10] before. The calculation of Ref. [10] is based on a Hamiltonian approach and takes final state interaction in the pion-nucleon system into account. The results of Ref. [10] are qualitatively reproduced in Fig. 4 by the field theoretic model of this
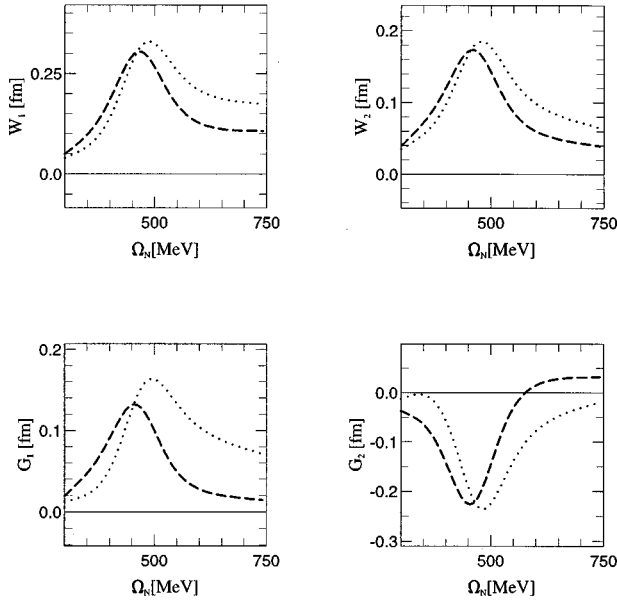
FIG. 5. Nucleonic structure functions $W_i^{N(t_N)}$ and $G_i^{N(t_N)}$ in the kinematic regime of pion production as functions of the energy transfer $\Omega_N = Q_N \cdot p_N / m_N$. The displayed results refer to the momentum transfer $Q_N^2 = -0.25$ GeV^2. The proton and neutron structure functions are compared; they are indicated by dashed and dotted curves, respectively.

FIG. 6. ^{3}He structure functions W_i^A and G_i^A in the kinematic regime of pion production as functions of the energy transfer $\Omega = Q \cdot P_A / m_A$. The displayed results refer to the momentum transfer $Q^2 = -0.25$ GeV^2. The proton and neutron contributions are indicated by the dashed and dotted curves, respectively. The full lines represent the full result.

section. Though the results on $\sigma_{TL'}^p$ are of the same magnitude, they differ in sign compared to Ref. [10]; the reason is unexplained.

Section IV chooses $Q^2 = -0.25$ GeV^2 as an example for the calculation of ^{3}He structure functions and for the discussion of pion production from ^{3}He. Though the momentum transfers to the nucleus and the struck nucleon are different, i.e., $Q \neq Q_N$, the convolution relation (2.9) requires the nucleonic structure functions around $Q_N^2 \simeq Q^2$ as computational building block. Figure 5 displays the proton and neutron structure functions at $Q_N^2 = -0.25$ GeV^2 as function of the energy loss Ω_N. Pion production is dominated by the Δ resonance. All nucleonic structure functions peak around the energy corresponding to Δ-isobar production. Around resonance the nonresonant background processes of Fig. 3 are suppressed; they are, however, responsible for the difference of proton and neutron structure functions. Furthermore, the background processes become significant for the nucleonic structure functions at energy losses Ω_N about 100 MeV above resonance. In contrast, the nucleonic responses, displayed in Fig. 4 in form of the partial cross sections σ^p for the proton, are not always dominated by the Δ resonance. The longitudinal response $R_L^{N(t_N)}$ sees the background processes exclusively, the longitudinal-transverse interference response $R_{TL'}^{N(t_N)}$ depends on them heavily.

We note that the proton and neutron structure functions are of comparable size in the kinematic regime of pion production. This fact is quite different compared with quasielastic scattering whose description requires the elastic nucleonic charge form factors, being much larger for the proton than for the neutron.
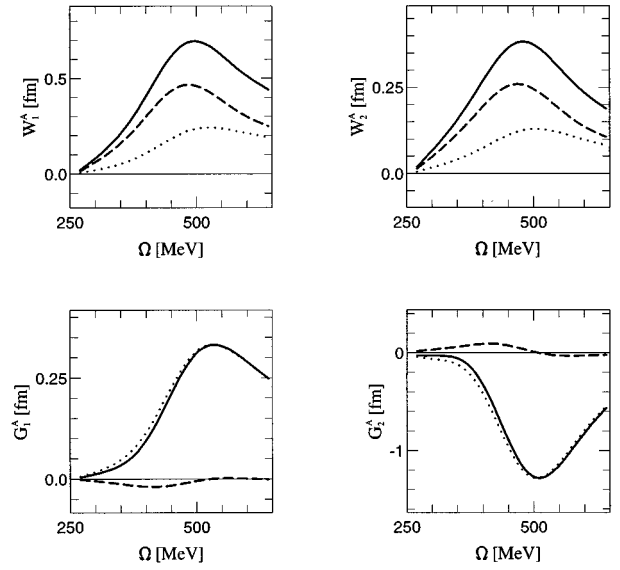
IV. ^{3}HE STRUCTURE FUNCTIONS FOR SINGLE-PION PRODUCTION AND CONCLUSIONS

Using the parametrization of the nucleonic structure functions for single-pion production in the convolution relation (2.9), ^{3}He structure functions are calculated. The often discussed quasielastic peak [3] occurs at $Q^0 = -Q^2/2m_N$. Correspondingly, pion production cross sections will be large when the P$_{33}$ pion-nucleon resonance, the Δ resonance, gets excited in the nucleus. Denoting the position of the resonance at 1232 MeV by m_Δ, the quasielastic Δ-resonance production peak of inelastic electron scattering occurs at

$$Q^0 = (m_\Delta - m_N)\left[1 + \frac{m_\Delta - m_N}{2m_N}\right] - \frac{Q^2}{2m_N}. \qquad (4.1)$$

The four ^{3}He structure functions are calculated in the regime of pion production. They are shown in Fig. 6 for the momentum transfer $Q^2 = -0.25$ GeV^2 as function of the energy transfer $\Omega = Q^0$. Figure 7 displays the corresponding spin-dependent nuclear responses. The proton and neutron contributions are indicated. Whereas proton and neutron make comparable contributions to the spin-averaged structure functions W_1^A and W_2^A, the spin-dependent structure functions G_1^A and G_2^A and the spin-dependent responses $R_{T'}^A$ and $R_{TL'}^A$ are dominated by the neutron. This fact is readily understood: The ^{3}He spin is largely carried by the neutron, only a minor part by the proton. Since e.m. pion production from proton and neutron is rather similar in size, the proton can contribute only little to the ^{3}He spin-dependent structure functions. Since the ^{3}He spin-dependent structure functions are dominated by the neutron, the neutron structure functions G_1^n and G_2^n can get unfolded from experimental ^{3}He data, with n standing for the label $N(-1/2)$. Indeed, polarized
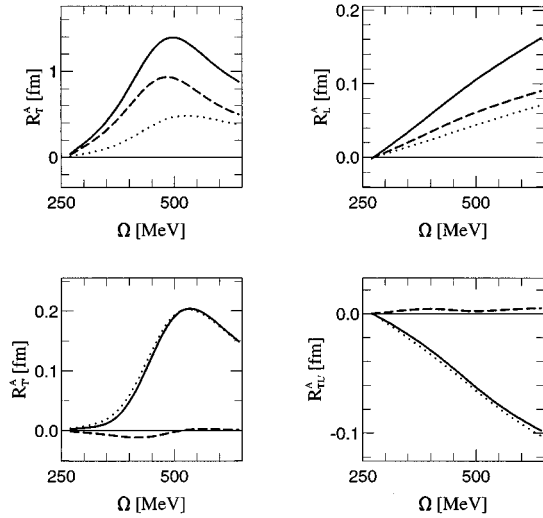
FIG. 7. ^{3}He responses R_i^A in the kinematic regime of pion production as functions of the energy transfer $\Omega = Q \cdot P_A / m_A$. The displayed results refer to the momentum transfer $Q^2 = -0.25$ GeV^2. The proton and neutron contributions are indicated by the dashed and dotted curves, respectively. The full lines represent the full result.

^{3}He appears — in the kinematic regime of pion production — to be an efficient substitute for unavailable neutron spin targets. This conclusion is in contrast to the one found for quasielastic scattering. We note that for the chosen kinematics the spin-dependent structure functions and responses do not reflect the same functional behavior. This observation in pion production is also in contrast to the situation discussed in the case of quasielastic scattering for which $R_{TL'}^A \propto G_1^A$ and $R_{T'}^A \propto G_2^A$ according to Ref. [3].
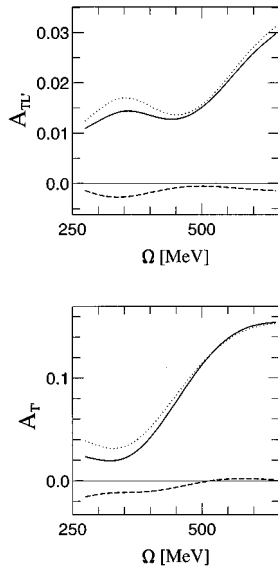

FIG. 8. Transverse-longitudinal and transverse asymmetries $A_{TL'}$ and $A_{T'}$ in the kinematic regime of pion production as functions of energy transfer $\Omega = Q \cdot P_A / m_A$. The displayed results refer to the momentum transfer $Q^2 = -0.25$ GeV^2 and the beam energy $k_e^0 = 0.88$ GeV. The proton and neutron contributions are indicated by the dashed and dotted curves, respectively. The full lines represent the full result.
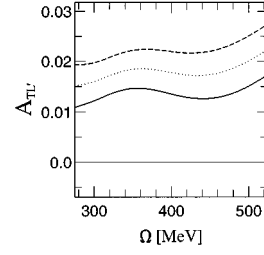

FIG. 9. Transverse-longitudinal asymmetry $A_{TL'}$ in the kinematic regime of pion production as functions of the energy transfer $\Omega = Q \cdot P_A / m_A$. The displayed results refer to the momentum transfer $Q^2 = -0.25$ GeV^2 and the beam energy $k_e^0 = 0.88$ GeV. The sensitivity with respect to the transition form factor G_C is displayed. The choices $G_C(0) = 0.25, 0, -0.25$ refer to the solid, dotted, and dashed curves, respectively.

The conclusion that polarized ^{3}He is an efficient substitute for a neutron spin target is confirmed for spin-dependent cross sections. The asymmetry A is defined by

$$A(k_e'^0, \Omega_e', \hat{\mathbf{n}}_A)$$

$$= \frac{d^2\sigma/dk_e'^0 d\Omega_e'(1, \hat{\mathbf{n}}_A) - d^2\sigma/dk_e'^0 d\Omega_e'(-1, \hat{\mathbf{n}}_A)}{d^2\sigma/dk_e'^0 d\Omega_e'(1, \hat{\mathbf{n}}_A) + d^2\sigma/dk_e'^0 d\Omega_e'(-1, \hat{\mathbf{n}}_A)}. \quad (4.2)$$

The asymmetry is called transverse-longitudinal, i.e., $A_{TL'}$, when the polarization angles are $(\theta^* = \pi/2, \phi^* = 0)$; it is called transverse, i.e., $A_{T'}$, when the polarization angles are $(\theta^* = 0, \phi^* = 0)$. Figure 8 shows that in both cases the asymmetry is dominated by the neutron contribution.

The nuclear response $R_{TL'}^A$ and the corresponding asymmetry $A_{TL'}$ are determined by the interference of charge and spatial current; the quantities depend sensitively on the charge form factor G_C for Δ-isobar excitation; the employed parametrization of G_C is given in Eq. (C.10c) of Appendix C of Ref. [6]; it is denoted there by G_C^*. Figure 9 shows the sensitivity of the asymmetry $A_{TL'}$ on G_C; thus, a measurement of $A_{TL'}$ may also serve as a method for determining properties of that form factor.

We conclude that a measurement of inclusive inelastic scattering from polarized ^{3}He in the region of pion production may efficiently yield information on neutron properties, more generally, on nucleon properties in pion production.

[1] *Electromagnetic Probes and the Structure of Hadrons and Nuclei*, edited by A. Faessler, Prog. Part. Nucl. Phys. **34** (Pergamon, Oxford, 1995).

[2] E. W. Otten, Prog. Part. Nucl. Phys. **24**, 103 (1990).

[3] R.-W. Schulze and P. U. Sauer, Phys. Rev. C **48**, 38 (1993).

[4] H. J. Lipkin and T.-S. H. Lee, Phys. Lett. B **183**, 22 (1987).

[5] H. Meier-Hajduk, Ch. Hajduk, P. U. Sauer, and W. Theis, Nucl. Phys. **A395**, 332 (1982).

[6] H. Meier-Hajduk, U. Oelfke, and P. U. Sauer, Nucl. Phys. **A499**, 637 (1989).

[7] C. Ciofi degli Atti, E. Pace, and G. Salmè, Phys. Lett. **141B**, 14 (1984).

[8] R.-W. Schulze, Ph.D. Thesis, University of Hannover, 1994.

[9] K. Bätzner *et al.*, Phys. Lett. **39B**, 575 (1972).

[10] S. Nozawa, B. Blankleider, and T.-S. H. Lee, Nucl. Phys. **A513**, 459 (1990); **A513**, 511 (1990); **A513**, 543 (1990).